

Structural and electrochemical study of $\text{Li}[\text{Cr}_x\text{Li}_{(1-x)/3}\text{Mn}_{2(1-x)/3}]\text{O}_2$ ($0 \leq x \leq 0.328$) cathode materials

C.W. Park^a, S.H. Kim^a, K.S. Nahm^b, H.T. Chung^c, Y.S. Lee^d, J.H. Lee^e, S. Boo^e, J. Kim^{a,*}

^a Department of Materials Science and Engineering, Chonnam National University, Gwangju 500-757, South Korea

^b School of Chemical Engineering and Technology, Chonbuk National University, Jeonju 561-756, South Korea

^c Department of Ceramic Engineering, Dongshin University, Naju 520-714, South Korea

^d School of Applied Chemical Engineering, Chonnam National University, Gwangju 500-757, South Korea

^e Energy & Applied Optics Team, Gwangju Research Center Korea Institute of Industrial Technology, Gwangju 500-460, South Korea

Received 4 November 2005; received in revised form 3 January 2006; accepted 10 January 2006

Available online 12 January 2007

Abstract

$\text{Li}[\text{Cr}_x\text{Li}_{(1-x)/3}\text{Mn}_{2(1-x)/3}]\text{O}_2$ with $x=0, 0.05, 0.1$ and 0.328 were synthesized by a solution method with subsequent quenching. The structures were investigated by X-ray diffraction (XRD), Rietveld refinement, electron diffraction and HRTEM. $\text{Li}[\text{Cr}_x\text{Li}_{(1-x)/3}\text{Mn}_{2(1-x)/3}]\text{O}_2$ ($x=0$ and 0.05) and annealed $\text{Li}[\text{Li}_{1/3}\text{Mn}_{2/3}]\text{O}_2$ were indexed based on the monoclinic structure, while $\text{Li}_{1.2}\text{Cr}_{0.4}\text{Mn}_{0.4}\text{O}_2$ was shown to be that of a nanocomposite. $\text{Li}[\text{Cr}_{0.1}\text{Li}_{0.29}\text{Mn}_{0.602}]\text{O}_2$ material formed based on the stoichiometry in between $\text{Li}[\text{Li}_{1/3}\text{Mn}_{2/3}]\text{O}_2$ and $\text{Li}[\text{Cr}_{0.328}\text{Li}_{0.22}\text{Mn}_{0.436}]\text{O}_2$ showed both sides features of the monoclinic and hexagonal structures in a nanocomposite structure and provided the lack of a developed anodic peak between 4.6 and 4.9 V, a good reversible capacity of around 250 mAh/g in a discharge voltage range between 2.8 and 3.5 V.

© 2006 Elsevier B.V. All rights reserved.

Keywords: Lithium batteries; Monoclinic; Layered compound; Manganese; Chromium

1. Introduction

LiMn_2O_4 suffers from capacity fading due to the dissolution of manganese [1] and Jahn–Teller distortion [2]. Besides, layered LiMnO_2 transforms into a spinel structure during the lithium insertion/extraction process, due to cation migration [3]. In order to obtain compounds with prolonged structural integrities, derivative layered manganese oxides [4–8] and lithium-saturated solid solutions or nanocomposite Li_2MnO_3 – LiMO_2 [9–13] have been investigated which also exhibit enhanced electrochemical performances.

$\text{Li}_{1.2}\text{Cr}_{0.4}\text{Mn}_{0.4}\text{O}_2$ shows relatively high capacity and cycling stability [14]. During cycling, chromium is redoxed between the octahedral sites (3+ state) and tetrahedral sites (6+ state) [15], while manganese in the 4+ oxidation state is embedded in an inert Li_2MnO_3 -like framework which maintains the structural stability. It is generally believed that Mn cannot be oxidized beyond +4 in an octahedrally coordinated environment [16]. Lu

and Dahn reported the synthesis of $\text{Li}[\text{Cr}_x\text{Li}_{(1-x)/3}\text{Mn}_{2(1-x)/3}]\text{O}_2$ ($0 \leq x \leq 1$) materials by the sol–gel method with heat treatment in an argon atmosphere [17]. When the amount of chromium is less than 0.5, Cr^{3+} is embedded in layered $\text{Li}[\text{Li}_{1/3}\text{Mn}_{2/3}]\text{O}_2$. Of the compounds which are formed in this manner, $\text{Li}[\text{Cr}_x\text{Li}_{(1-x)/3}\text{Mn}_{2(1-x)/3}]\text{O}_2$ ($x=1/6$) delivers a reversible capacity of about 230 mAh/g. Manganese-rich $\text{Li}[\text{Ni}_x\text{Li}_{(1-2x)/3}\text{Mn}_{(2-x)/3}]\text{O}_2$ ($x \leq 1/3$) prepared by quenching shows a slightly higher capacity and cycling stability than a slowly cooled sample [18]. The quenching process enhances the capacity and cyclability. Thackeray *et al.* classified $\text{Li}_{1.2}\text{Cr}_{0.4}\text{Mn}_{0.4}\text{O}_2$ as $(0.4)\text{Li}_2\text{MnO}_3 \cdot (0.4)\text{LiCrO}_2$ and reported the synthesis of composite $x\text{Li}_2\text{MnO}_3 \cdot (1-x)\text{LiMn}_{0.5}\text{Ni}_{0.5}\text{O}_2$ electrodes which form nanocomposite Li_2MnO_3 – LiMO_2 structures with nanometer regions with Li_2MnO_3 - and LiMO_2 -like features, confirming the composite character of these materials [19].

The objective of the present work is to synthesize $\text{Li}[\text{Cr}_x\text{Li}_{(1-x)/3}\text{Mn}_{2(1-x)/3}]\text{O}_2$ ($x=0, 0.05, 0.1$ and 0.328) using a solution method with a subsequent quenching process. In particular, we focus on the characterization of the crystal structure with respect to the Cr:Mn ratio and electrochemical prop-

* Corresponding author. Tel.: +82 62 530 1703; fax: +82 62 530 1699.
 E-mail address: jaekook@chonnam.ac.kr (J. Kim).

Table 1

Inductively coupled plasma (ICP) analysis of washed $\text{Li}[\text{Li}_{1/3}\text{Mn}_{2/3}]\text{O}_2$, $\text{Li}[\text{Cr}_{0.1}\text{Li}_{0.3}\text{Mn}_{0.6}]\text{O}_2$, $\text{Li}[\text{Cr}_{0.2}\text{Li}_{0.266}\text{Mn}_{0.533}]\text{O}_2$ and $\text{Li}[\text{Cr}_{0.4}\text{Li}_{0.2}\text{Mn}_{0.4}]\text{O}_2$

Target stoichiometry	Measured stoichiometry (Ref. O = 2)			
	Li	Cr	Mn	O
$\text{Li}[\text{Li}_{1/3}\text{Mn}_{2/3}]\text{O}_2$	1.335	–	0.665	2
$\text{Li}[\text{Cr}_{0.1}\text{Li}_{0.3}\text{Mn}_{0.6}]\text{O}_2$	1.32	0.05	0.63	2
$\text{Li}[\text{Cr}_{0.2}\text{Li}_{0.266}\text{Mn}_{0.533}]\text{O}_2$	1.29	0.1	0.602	2
$\text{Li}[\text{Cr}_{0.4}\text{Li}_{0.2}\text{Mn}_{0.4}]\text{O}_2$	1.22	0.328	0.436	2

erties of $\text{Li}[\text{Cr}_x\text{Li}_{(1-x)/3}\text{Mn}_{2(1-x)/3}]\text{O}_2$ (where $x=0, 0.05, 0.1$ and 0.328).

2. Experimental

$\text{Li}[\text{Cr}_x\text{Li}_{(1-x)/3}\text{Mn}_{2(1-x)/3}]\text{O}_2$ (where $x=0, 0.05, 0.1$ and 0.328) materials were prepared by mixing appropriate molar ratios of chromium acetate, manganese acetate and lithium hydroxide. A 100 mL aqueous solution of $\text{LiOH}\cdot\text{H}_2\text{O}$ was slowly dripped into a 100 mL pre-dissolved solution of the transition-metal acetates. Stirring was continued for 24 h to ensure a homogeneous reaction. The solution was dried in air until it became a gel. The gel thus obtained was heated initially in an oven at 110°C for 6 h, and then ground and heated at 600°C for 3 h. Finally, the powders were fired at 900°C for 12 h and quenched using two copper plates. An annealed version of $\text{Li}[\text{Li}_{1/3}\text{Mn}_{2/3}]\text{O}_2$ was prepared with a cooling rate of $5^\circ\text{C}/\text{min}$, in order to compare it with the quenched $\text{Li}[\text{Li}_{1/3}\text{Mn}_{2/3}]\text{O}_2$ sample. The prepared samples were washed with distilled water to remove Li_2CrO_4 and then dried in a vacuum at 100°C [20].

The elemental composition of the prepared cathode powders was determined by inductively coupled plasma (ICP) analysis, using a Perkin-Elmer 4300 DV analyzer. The thermogravimetric analysis (TGA) of the precursor powder was conducted on an SDT Q600 V8.0 Build 95 thermal analyzer at a heating rate of $10^\circ\text{C}/\text{min}$ from room temperature to 900°C in air. The crystallinity of the powders was measured by X-ray diffraction (XRD) using a D/MAX Ultima III diffractometer (Rigaku, Japan) with $\text{Cu K}\alpha$ radiation ($\lambda = 1.54056 \text{ \AA}$) and the lattice parameters were derived using the Rietveld method. A detailed analysis of the crystallinity was conducted by examining the transmission electron microscope (TEM) spot patterns, and TEM images were collected on a JEOL-JEM 2000FX-II transmission electron microscope under an accelerating voltage of 200 KeV. High-resolution TEM images of the powders were collected on a Philips-Tecna F20 transmission electron microscope. The morphology of the samples was examined by field emission scanning electron microscopy (FESEM) using a Hitachi S4700 instrument.

The electrochemical performances of the prepared cathode materials were tested in a battery tester system 2004. The cathode contained the active material, and tetra acetylene black as a conductor combined with a binder at a weight ratio of 58:42. An electrolyte consisting of a 1 M solution of LiPF_6 in ethylene carbonate (EC) and dimethyl carbonate (DMC) (1:1, v/v) and the prepared cathode were assembled in an argon filled glove box. The cells were tested in the voltage range of 4.9–2.4 V.

3. Results and discussion

Table 1 shows the inductively coupled plasma analysis results for the $\text{Li}[\text{Li}_{1/3}\text{Mn}_{2/3}]\text{O}_2$, $\text{Li}[\text{Cr}_{0.1}\text{Li}_{0.3}\text{Mn}_{0.6}]\text{O}_2$, $\text{Li}[\text{Cr}_{0.2}\text{Li}_{0.266}\text{Mn}_{0.533}]\text{O}_2$ and $\text{Li}[\text{Cr}_{0.4}\text{Li}_{0.2}\text{Mn}_{0.4}]\text{O}_2$ powders. Compared to that of the samples designed to act as the stoichiometrically calculated target samples, the chromium content in the washed $\text{Li}[\text{Cr}_x\text{Li}_{(1-x)/3}\text{Mn}_{2(1-x)/3}]\text{O}_2$ ($x=0.1, 0.2$ and 0.4) was decreased. In the thermogravimetric analysis, the weight percent of $\text{Li}[\text{Cr}_{0.4}\text{Li}_{0.2}\text{Mn}_{0.4}]\text{O}_2$ increases between 550 and 650°C , which means that the oxidation state of

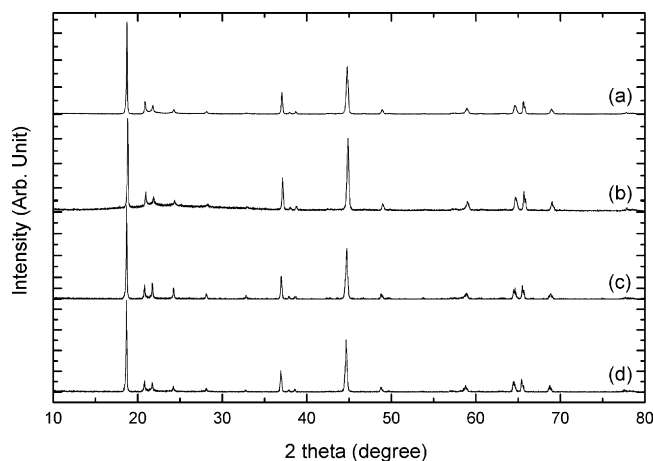


Fig. 1. X-ray diffraction patterns of: (a) slowly cooled $\text{Li}[\text{Li}_{1/3}\text{Mn}_{2/3}]\text{O}_2$, (b) $\text{Li}[\text{Li}_{1/3}\text{Mn}_{2/3}]\text{O}_2$, (c) $\text{Li}[\text{Cr}_{0.1}\text{Li}_{0.3}\text{Mn}_{0.6}]\text{O}_2$ and (d) $\text{Li}[\text{Cr}_{0.2}\text{Li}_{0.266}\text{Mn}_{0.533}]\text{O}_2$ which adopt the stoichiometries of Li_2MnO_3 , $\text{Li}_{1.95}\text{Cr}_{0.15}\text{Mn}_{0.9}\text{O}_3$ and $\text{Li}_{1.9}\text{Cr}_{0.3}\text{Mn}_{0.8}\text{O}_3$, respectively.

some of the Cr ions is increased to 6+. Hence, Li_2CrO_4 is easily generated in an air atmosphere. However, the generation of Li_2CrO_4 has not previously been reported in an inert atmosphere, due to the insufficiency of the oxygen supply [6,16–17]. The decrease in the chromium content indicated by the inductively coupled plasma results was confirmed by the X-ray diffraction study which shows the Li_2CrO_4 peaks in the unwashed $\text{Li}[\text{Cr}_{0.4}\text{Li}_{0.2}\text{Mn}_{0.4}]\text{O}_2$ disappeared in the washed $\text{Li}[\text{Cr}_{0.4}\text{Li}_{0.2}\text{Mn}_{0.4}]\text{O}_2$. This observation suggests that obtaining the target stoichiometry is difficult in an air atmosphere, due to the generation of Li_2CrO_4 , and it is difficult to accurately determine the amount of chromium removed. Therefore, more extensive research is needed to reveal the mechanism by which Li_2CrO_4 is generated.

Fig. 1 shows the X-ray diffraction patterns of $\text{Li}[\text{Cr}_x\text{Li}_{(1-x)/3}\text{Mn}_{2(1-x)/3}]\text{O}_2$ ($x=0, 0.05$ and 0.1) and the annealed $\text{Li}[\text{Li}_{1/3}\text{Mn}_{2/3}]\text{O}_2$. According to the results from Rietveld refinement, all of the patterns correspond more closely to a monoclinic structure with space group $C2/C$ than to a hexagonal structure, as determined by comparing them with the broadened superlattice peaks of the hexagonal $\alpha\text{-NaFeO}_2$ structure shown in Fig. 2b. To confirm the structural differences between the annealed and quenched $\text{Li}[\text{Li}_{1/3}\text{Mn}_{2/3}]\text{O}_2$, the lattice parameters were derived. The measured values of the GOF for the annealed and quenched $\text{Li}[\text{Li}_{1/3}\text{Mn}_{2/3}]\text{O}_2$, which indicates the proportion of coincidence, were 1.3 and 1.1, respectively. These data suggest that the annealed $\text{Li}[\text{Li}_{1/3}\text{Mn}_{2/3}]\text{O}_2$ more closely coincided with a monoclinic structure than the quenched sample. The values of R_B of 7.94 and 9.82, respectively, also support these results. According to Yoon *et al.*, the use of a rapid cooling rate restricts the diffusivities of cations such as Li and Mn at the order/disorder transition temperature of approximately 1000 K [21]. This observation suggests that the quenched $\text{Li}[\text{Li}_{1/3}\text{Mn}_{2/3}]\text{O}_2$ develops defects and poor crystallinity more easily than the annealed $\text{Li}[\text{Li}_{1/3}\text{Mn}_{2/3}]\text{O}_2$. The defects of the quenched $\text{Li}[\text{Li}_{1/3}\text{Mn}_{2/3}]\text{O}_2$ observed in the

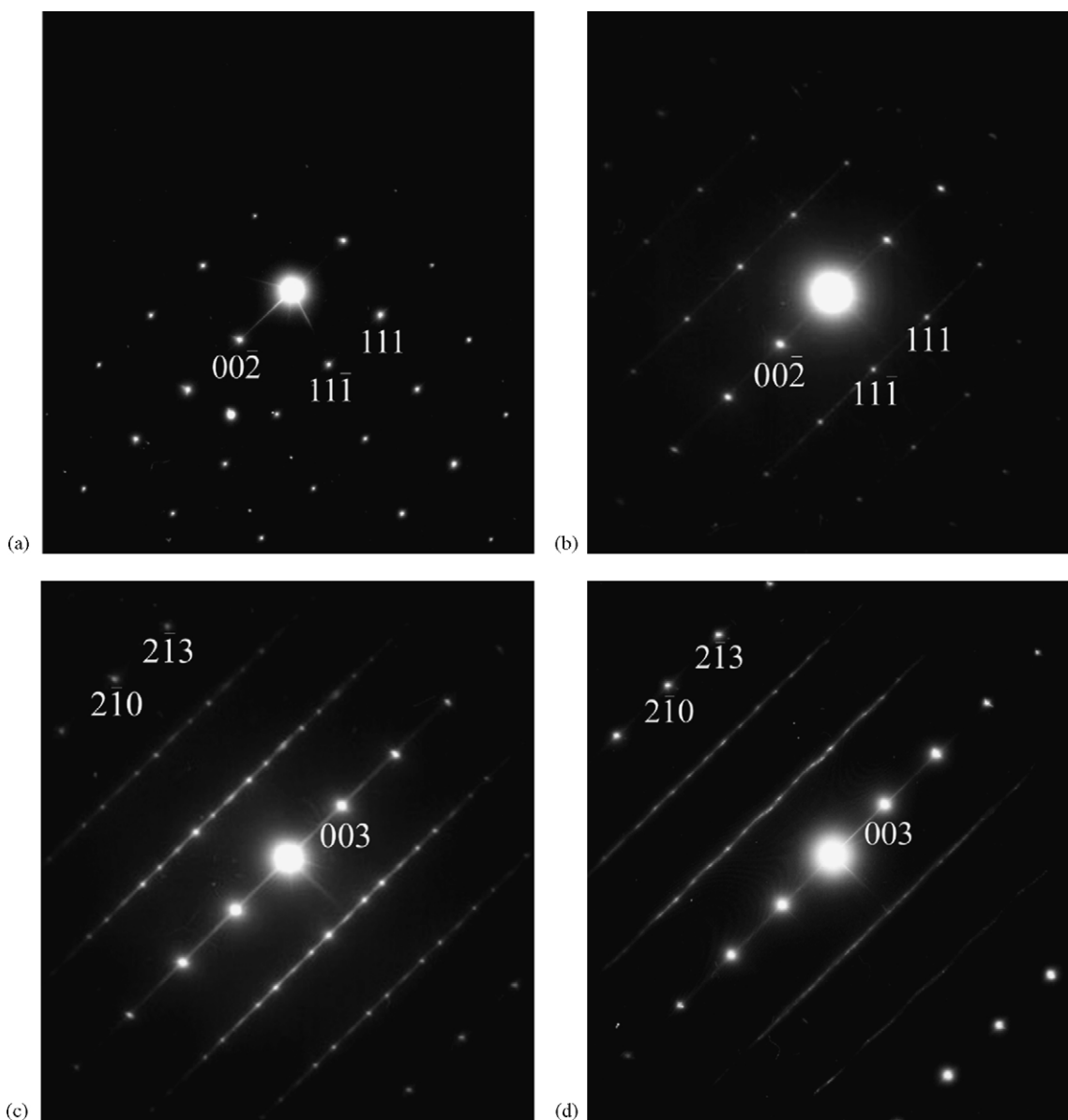


Fig. 2. TEM electron diffraction pattern of monoclinic phase in $[1\ 1\ 0]$ zone from the: (a) $\text{Li}_{1.95}\text{Cr}_{0.15}\text{Mn}_{0.9}\text{O}_3$, (b) $\text{Li}_{1.9}\text{Cr}_{0.3}\text{Mn}_{0.8}\text{O}_3$, (c) tilted $\text{Li}_{1.9}\text{Cr}_{0.3}\text{Mn}_{0.8}\text{O}_3$ powder and (d) rhombohedral phase in $[1\ 2\ 0]$ zone from the $\text{Li}[\text{Cr}_{0.4}\text{Li}_{0.2}\text{Mn}_{0.4}]\text{O}_2$ powder calcined at 900°C prior to cycling.

HRTEM image and the electrochemical differences between the annealed and quenched $\text{Li}[\text{Li}_{1/3}\text{Mn}_{2/3}]\text{O}_2$ are discussed below.

Fig. 2a shows the electron diffraction pattern of the monoclinic structure in the $[1\ 1\ 0]$ zone obtained from the $\text{Li}[\text{Cr}_{0.05}\text{Li}_{0.32}\text{Mn}_{0.63}]\text{O}_2$ powder. Fig. 2b and c show the electron diffraction patterns of the monoclinic phase in the $[1\ 1\ 0]$ zone obtained from the $\text{Li}[\text{Cr}_{0.1}\text{Li}_{0.29}\text{Mn}_{0.6}]\text{O}_2$ powder and the slightly tilted $\text{Li}[\text{Cr}_{0.1}\text{Li}_{0.29}\text{Mn}_{0.6}]\text{O}_2$ powder, respectively. Fig. 2d shows the electron diffraction pattern of the hexagonal phase in the $[1\ 2\ 0]$ zone obtained from the $\text{Li}[\text{Cr}_{0.328}\text{Li}_{0.22}\text{Mn}_{0.436}]\text{O}_2$ powder. It is well known that the $[1\ 1\ 0]$ zone of the monoclinic structure coexists with the $[1\ 1\ 1]$ zone of the hexagonal structure. These data suggest the possibility of making a nano district composite formed by the monoclinic structure of solid solution limits as $\text{Li}_{2-x}[\text{Cr}_{3x}\text{Mn}_{1-x}]\text{O}_3$ and the

hexagonal structure of the solid solution as $\text{Li}[\text{Cr}_x\text{Mn}_{(1-x)}]\text{O}_2$. However, it is difficult to accurately determine the amount of chromium in the solid solution, which cleaves from the nano district composite. At a chromium amount of more than that of $\text{Li}[\text{Cr}_{0.1}\text{Li}_{0.29}\text{Mn}_{0.6}]\text{O}_2$, the property of a nanocomposite was observed. Hence, $\text{Li}[\text{Cr}_{0.1}\text{Li}_{0.29}\text{Mn}_{0.6}]\text{O}_2$ and $\text{Li}[\text{Cr}_{0.4}\text{Li}_{0.2}\text{Mn}_{0.4}]\text{O}_2$ can be represented as $x\text{Li}_{2-x'}[\text{Cr}_{3x'}\text{Mn}_{1-x'}]\text{O}_3 \cdot (1-x)\text{Li}[\text{Cr}_{x'}\text{Mn}_{(1-x'')}\text{O}_2$.

With regard to the amount of chromium, the formation of either the solid solution or the nano district composite was verified by examining the HRTEM images. Fig. 3 shows the HRTEM images of $\text{Li}[\text{Cr}_{0.05}\text{Li}_{0.32}\text{Mn}_{0.63}]\text{O}_2$ and $\text{Li}[\text{Cr}_{0.328}\text{Li}_{0.22}\text{Mn}_{0.436}]\text{O}_2$, respectively. Throughout the primary particles, Fig. 3a shows that the monoclinic $(1\ 1\ 1)$ planes are aligned. However, Fig. 3b shows that the $(0\ 2\ 1)$ planes, the $(2\ 2\ 1)$ planes of the monoclinic structure and the $(2\ 0\ 2)$

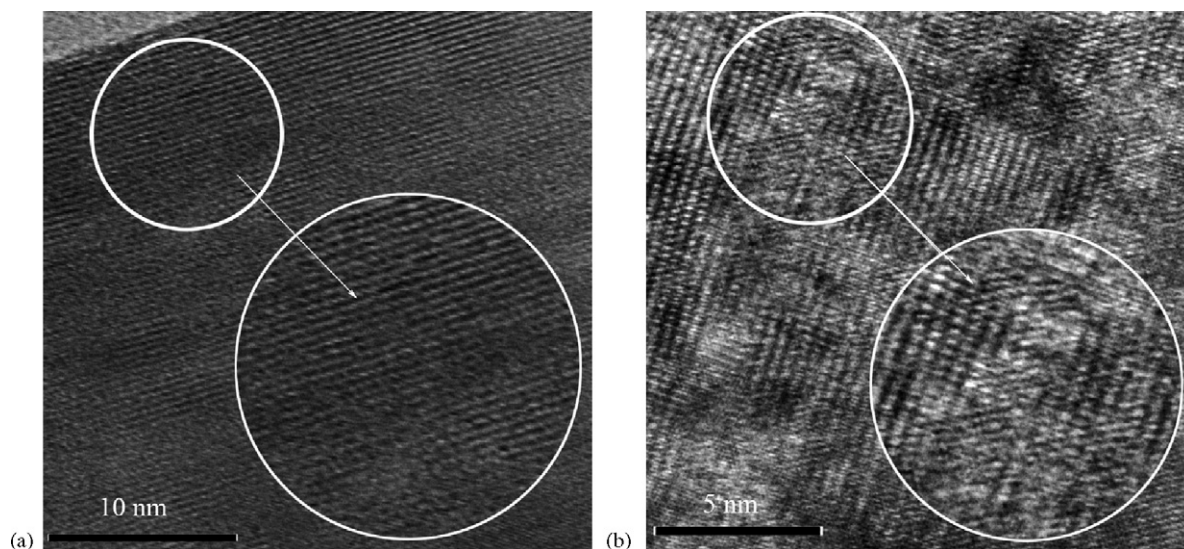


Fig. 3. HRTEM images of: (a) $\text{Li}_{1.95}\text{Cr}_{0.15}\text{Mn}_{0.9}\text{O}_3$ and (b) $\text{Li}[\text{Cr}_{0.4}\text{Li}_{0.2}\text{Mn}_{0.4}]\text{O}_2$ which both adopt the stoichiometry of $x\text{Li}_{2-y}[\text{Cr}_3\text{yMn}_{1-y}]\text{O}_3 \cdot (1-x)\text{LiCrO}_2$.

planes of the hexagonal structure are concurrently aligned and conform to the nano domain in the primary particles. These figures reveal that, above a certain critical amount of chromium, $\text{Li}[\text{Cr}_x\text{Li}_{(1-x)/3}\text{Mn}_{2(1-x)/3}]\text{O}_2$ were made by nanocomposite. As shown in Fig. 3a and b, distorted and defected lattices are shown in both structures. In particular, many defects are observed in $\text{Li}[\text{Cr}_{0.328}\text{Li}_{0.22}\text{Mn}_{0.436}]\text{O}_2$ due to the removal of Li_2CrO_4 and the quenching effect.

The morphologies of $\text{Li}[\text{Cr}_x\text{Li}_{(1-x)/3}\text{Mn}_{2(1-x)/3}]\text{O}_2$ ($x=0, 0.05, 0.1$ and 0.328) and the annealed $\text{Li}[\text{Li}_{1/3}\text{Mn}_{2/3}]\text{O}_2$ are shown in Fig. 4. The average crystal size of the annealed $\text{Li}[\text{Li}_{1/3}\text{Mn}_{2/3}]\text{O}_2$, quenched Li_2MnO_3 , $\text{Li}[\text{Cr}_{0.05}\text{Li}_{0.32}\text{Mn}_{0.63}]\text{O}_2$, $\text{Li}[\text{Cr}_{0.1}\text{Li}_{0.29}\text{Mn}_{0.6}]\text{O}_2$ and $\text{Li}[\text{Cr}_{0.328}\text{Li}_{0.22}\text{Mn}_{0.436}]\text{O}_2$ are 1, 0.7, 0.35, 0.4 and $0.25\ \mu\text{m}$, respectively. By comparing Fig. 4a with b, it can be seen that the quenching increases the roughness of the particle surface and decreases

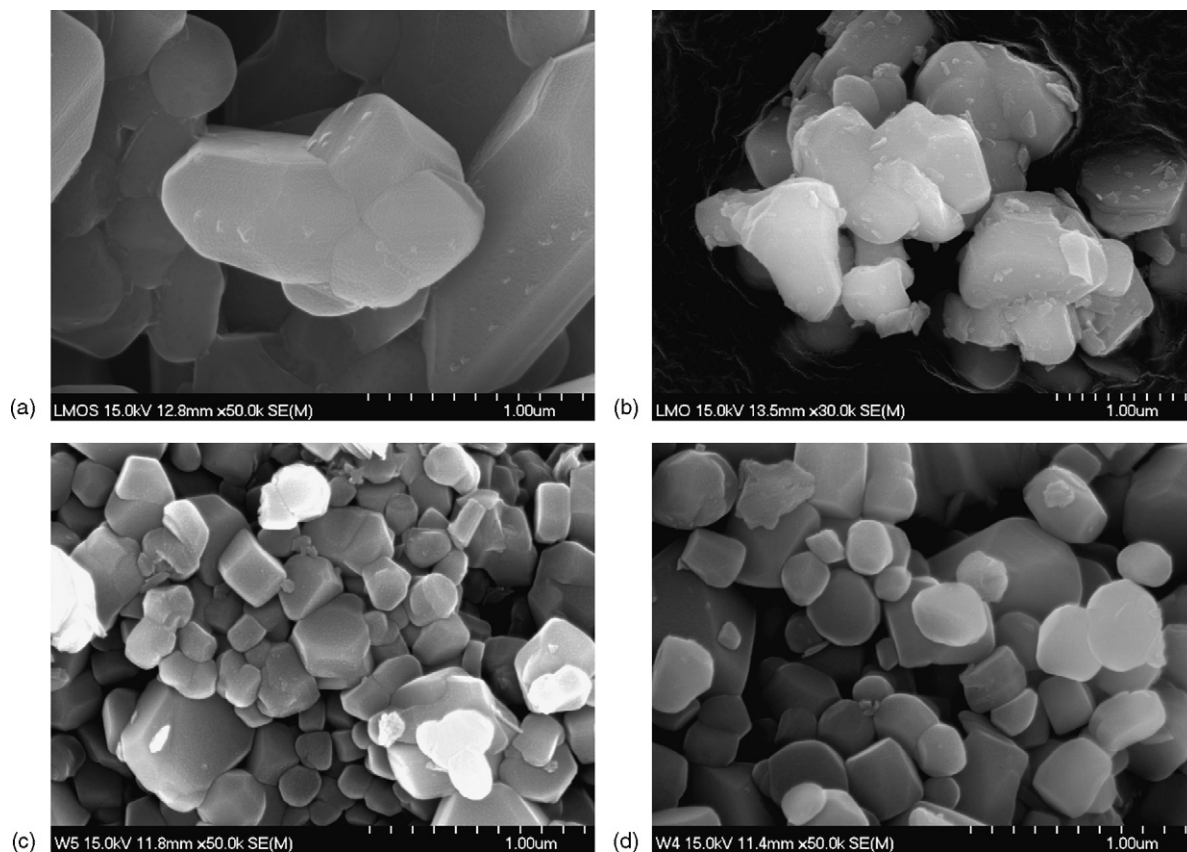


Fig. 4. Scanning electron micrograph (SEM) images of: (a) slow cooled Li_2MnO_3 , (b) quenched Li_2MnO_3 , (c) $\text{Li}_{1.95}\text{Cr}_{0.15}\text{Mn}_{0.9}\text{O}_3$ and (d) $\text{Li}_{1.9}\text{Cr}_{0.3}\text{Mn}_{0.8}\text{O}_3$.

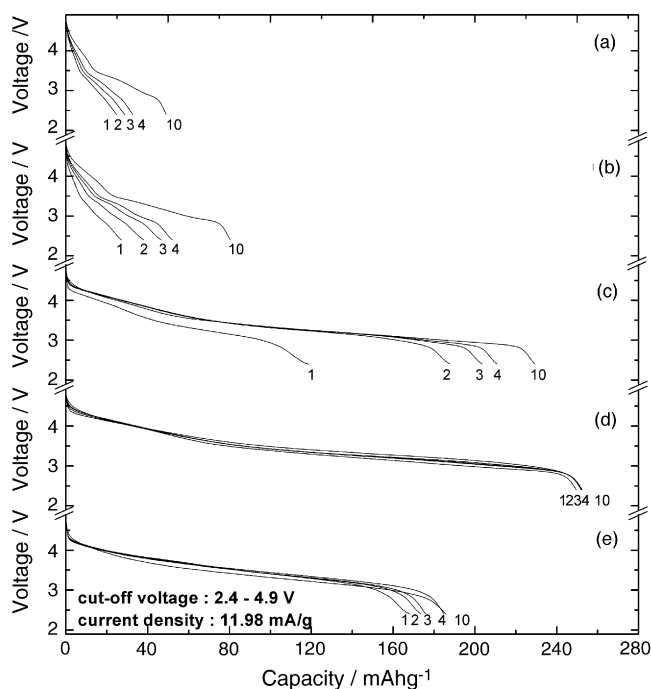


Fig. 5. Discharge curves of: (a) slow cooled Li_2MnO_3 , (b) quenched Li_2MnO_3 , (c) $\text{Li}_{1.95}\text{Cr}_{0.15}\text{Mn}_{0.9}\text{O}_3$, (d) $\text{Li}_{1.9}\text{Cr}_{0.3}\text{Mn}_{0.8}\text{O}_3$ and (e) $\text{Li}[\text{Cr}_{0.4}\text{Li}_{0.2}\text{Mn}_{0.4}]\text{O}_2$.

the particle size. Increasing the Cr content causes a decrease in the particle size and enhances the uniformity of the particles.

Fig. 5 shows the discharge curves of the quenched $\text{Li}[\text{Li}_{1/3}\text{Mn}_{2/3}]\text{O}_2$, $\text{Li}[\text{Cr}_{0.05}\text{Li}_{0.32}\text{Mn}_{0.63}]\text{O}_2$, $\text{Li}[\text{Cr}_{0.1}\text{Li}_{0.29}\text{Mn}_{0.6}]\text{O}_2$, $\text{Li}[\text{Cr}_{0.328}\text{Li}_{0.22}\text{Mn}_{0.436}]\text{O}_2$ and annealed $\text{Li}[\text{Li}_{1/3}\text{Mn}_{2/3}]\text{O}_2$ cells cycled between 2.4 and 4.9 V with a current density of 11.98 mA/g. In general, $\text{Li}[\text{Li}_{1/3}\text{Mn}_{2/3}]\text{O}_2$ is believed to be an inactive material, because the Mn^{4+} ion in $\text{Li}[\text{Li}_{1/3}\text{Mn}_{2/3}]\text{O}_2$ cannot be oxidized beyond the +4 oxidation state in order to extract Li. However, the inactive $\text{Li}[\text{Li}_{1/3}\text{Mn}_{2/3}]\text{O}_2$ could be activated by using acid treatment [22] or by charging it to a high potential [23]. The discharge curve of the annealed $\text{Li}[\text{Li}_{1/3}\text{Mn}_{2/3}]\text{O}_2$ in Fig. 5a shows the electrochemical properties which result from charging to a high potential. The discharge curve of the quenched $\text{Li}[\text{Li}_{1/3}\text{Mn}_{2/3}]\text{O}_2$ in Fig. 5b shows that its capacity is greater than that of the annealed $\text{Li}[\text{Li}_{1/3}\text{Mn}_{2/3}]\text{O}_2$. The extended capacity of $\text{Li}[\text{Li}_{1/3}\text{Mn}_{2/3}]\text{O}_2$ was attributed to the presence of defects and the poorly developed crystallinity, as verified by the Rietveld refinement and HRTEM imaging. In short, $\text{Li}[\text{Cr}_{0.1}\text{Li}_{0.29}\text{Mn}_{0.602}]\text{O}_2$ situated between monoclinic $\text{Li}[\text{Li}_{1/3}\text{Mn}_{2/3}]\text{O}_2$ and layered $\text{Li}[\text{Cr}_{0.328}\text{Li}_{0.22}\text{Mn}_{0.436}]\text{O}_2$ provides both sides features such as the lack of a developed anodic peak between 4.6 and 4.9 V, good reversible capacity of around 250 mAh g^{-1} and a discharge voltage range between 2.8 and 3.5 V. The discharge curve of $\text{Li}[\text{Cr}_{0.328}\text{Li}_{0.22}\text{Mn}_{0.436}]\text{O}_2$ shown in Fig. 5e demonstrates that it has relatively good reversible capacity. The discharge voltage range was distributed between 3.2 and 4.0 V and the peak with increasing intensity at around 3.2 V was not observed, which distinguished this cell from the $\text{Li}[\text{Cr}_x\text{Li}_{(1-x)/3}\text{Mn}_{2(1-x)/3}]\text{O}_2$ ($x=0, 0.05$) cells. Compared to the reversible capacity of $\text{Li}[\text{Cr}_{0.328}\text{Li}_{0.22}\text{Mn}_{0.436}]\text{O}_2$,

the reversible capacity of $\text{Li}[\text{Cr}_{0.1}\text{Li}_{0.29}\text{Mn}_{0.6}]\text{O}_2$, is slightly decreased, due to the increase in the amount of inactive LiCrO_2 in the solid solution of $\text{Li}[\text{Cr}_x\text{Mn}_{(1-x)}]\text{O}_2$. The present study was limited to observing the electrochemical tendency as a function of the chromium content. Therefore, more detailed electron state studies of $\text{Li}[\text{Cr}_x\text{Li}_{(1-x)/3}\text{Mn}_{2(1-x)/3}]\text{O}_2$ cells during cycling are needed, in order to reveal the precise charge/discharge mechanism.

4. Conclusions

$\text{Li}[\text{Cr}_x\text{Li}_{(1-x)/3}\text{Mn}_{2(1-x)/3}]\text{O}_2$ with $x=0, 0.05, 0.1$ and 0.328 were synthesized by a solution method and subsequent quenching process. However, obtaining the target stoichiometry is difficult, due to the generation of Li_2CrO_4 . $\text{Li}[\text{Cr}_x\text{Li}_{(1-x)/3}\text{Mn}_{2(1-x)/3}]\text{O}_2$ ($x=0$ and 0.05) were indexed based on the monoclinic structure and $\text{Li}[\text{Cr}_{0.328}\text{Li}_{0.22}\text{Mn}_{0.436}]\text{O}_2$ was indexed based on the rhombohedral structure. According to the HRTEM images, $\text{Li}[\text{Cr}_{0.328}\text{Li}_{0.22}\text{Mn}_{0.436}]\text{O}_2$ is composed of a nano district composite with a monoclinic structure of solid solution limits as $\text{Li}_{2-x}[\text{Cr}_x\text{Mn}_{1-x}]\text{O}_3$ and a hexagonal structure of solid solution as $\text{Li}[\text{Cr}_x\text{Mn}_{(1-x)}]\text{O}_2$. Hence, $\text{Li}[\text{Cr}_{0.328}\text{Li}_{0.22}\text{Mn}_{0.436}]\text{O}_2$ can be represented as $x\text{Li}_{2-x'}[\text{Cr}_{3x'}\text{Mn}_{1-x'}]\text{O}_3 \cdot (1-x)\text{Li}[\text{Cr}_{x''}\text{Mn}_{(1-x'')}] \text{O}_2$. However, it is difficult to determine the exact amount of chromium in the solid solution, which cleaves from the nano district composite. $\text{Li}[\text{Cr}_{0.1}\text{Li}_{0.29}\text{Mn}_{0.6}]\text{O}_2$ and $\text{Li}[\text{Cr}_{0.328}\text{Li}_{0.22}\text{Mn}_{0.436}]\text{O}_2$ provide good reversible capacities of around 250 and 180 mAh/g, respectively. As compared to the reversible capacity of $\text{Li}[\text{Cr}_{0.4}\text{Li}_{0.2}\text{Mn}_{0.4}]\text{O}_2$, that of $\text{Li}_{1.9}\text{Cr}_{0.3}\text{Mn}_{0.8}\text{O}_3$ is slightly decreased, due to the increase in the amount of inactive LiCrO_2 in the solid solution of $\text{Li}[\text{Cr}_x\text{Mn}_{(1-x)}]\text{O}_2$.

Acknowledgement

This work was supported by the Core Technology Development Program of the Ministry of Commerce, Industry and Energy (MOCIE).

References

- [1] S.J. Wen, T.J. Richardson, L. Ma, K.A. Striebel, P.N. Ross, E.J. Cairns, J. Electrochem. Soc. 143 (1996) L136.
- [2] M.M. Thackeray, Y. Shao-Horn, A.J. Kahaian, K.D. Kepler, E. Skinner, J.T. Vaughey, S.J. Hackney, Electrochem. Solid State Lett. 1 (1998) 7.
- [3] L. Croguennec, P. Deniard, R. Brec, J. Electrochem. Soc. 144 (1997) 3323.
- [4] I.J. Davidson, R.S. McMillan, J.J. Murray, J. Power Sources 54 (1995) 205.
- [5] Y.I. Jang, B. Huang, Y.M. Chiang, D.R. Sadoway, Electrochem. Solid State Lett. 1 (1998) 13.
- [6] B. Ammundsen, J. Desilvestro, T. Groutso, D. Hassell, J.B. Metson, E. Regan, R. Steiner, P.J. Pickering, J. Electrochem. Soc. 147 (2000) 4078.
- [7] A.R. Armstrong, R. Gitzendanner, A.D. Robertson, P.G. Bruce, Chem. Commun. (1998) 1833.
- [8] E. Rossen, C.D.W. Jones, J.R. Dahn, Solid State Ionics 57 (1992) 311.
- [9] M.H. Rossouw, M.M. Thackeray, Mater. Res. Bull. 26 (1991) 2864.
- [10] K. Numata, S. Yamanaka, Solid State Ionics 118 (1999) 117.
- [11] Z. Lu, L.Y. Beaulieu, R.A. Donabarger, C.L. Thomas, J.R. Dahn, J. Electrochem. Soc. 149 (2002) A778.

- [12] C. Storey, I. Kargina, Y. Grincourt, I.J. Davidson, Y. Yoo, D.Y. Seung, J. Power Sources 541 (2001) 97.
- [13] Y. Gincourt, C. Storey, I.J. Davidson, J. Power Sources 711 (2001) 97.
- [14] C. Storey, I. Kargina, Y. Grincourt, I.J. Davidson, Y. Yoo, D.Y. Seung, Proceedings of the 10th International Meeting on Lithium Batteries, Como, Italy, May 28–June 2, 2000 (Abstract No. 234).
- [15] Z.P. Guo, S. Zhong, G.X. Wang, G. Walter, H.K. Liu, S.X. Dou, J. Electrochem. Soc. 149 (2002) A792.
- [16] B. Ammundsen, J. Paulsen, J. Adv. Mater. 13 (2001) 943.
- [17] Z. Lu, J.R. Dahn, J. Electrochem. Soc. 149 (2002) A1454.
- [18] X. Wu, K.S. Ryu, Y.S. Hong, Y.J. Park, S.H. Chang, J. Power Sources 132 (2004) 219.
- [19] M.M. Thackeray, C.S. Johnson, J.T. Vaughey, N. Li, S.A. Hackney, J. Mater. Chem. 15 (2005) 2257.
- [20] K.S. Kim, S.W. Lee, H.S. Moon, H.J. Kim, B.W. Cho, W.I. Cho, J.B. Choi, J.W. Park, J. Power Sources 129 (2004) 319.
- [21] W.S. Yoon, S. Iannopolo, C.P. Grey, D. Carlier, J. Gorman, J. Reed, G. Ceder, Electrochem. Solid State Lett 7 (2004) A167.
- [22] M.H. Rossouw, M.M. Thackeray, Mater. Res. Bull. 26 (1991) 463.
- [23] P. Kalyani, S. Chitra, T. Mohan, S. Gopukumar, J. Power Sources 80 (1996) 103.